Special Issue

Tetrahydrothiophene-Based Ionic Liquids: Synthesis and Thermodynamic Characterizations

Alexa Schmitz,[a] Mark Bülow,[b] Dana Schmidt,[a] Dzmitry H. Zaitsau,[c, d] Fabian Junglas,[a] Tim-Oliver Knedel,[a] Sergey P. Verevkin,[c, d] Christoph Held,[b] and Christoph Janiak*[a]

S-alkyltetrahydrothiophenium, $[C_nTHT]^+$ bis(trifluorosulfonyl) imide, $[NTf_2]^-$ room temperature ionic liquids (ILs) and tetraphenylborate, $[BPh_4]^-$ salts with alkyl chain lengths from C_4 to C_{10} have been prepared. The ILs and salts were characterized and their purity verified by ^{1}H- and ^{13}C-nuclear magnetic resonance, elemental analysis, ion chromatography, Karl-Fischer titration, single crystal X-ray diffraction as well as thermogravimetric analysis. The experimentally determined density and viscosity decrease with increasing temperature. The experimental solubility of the $[C_nTHT][NTf_2]$-ILs in water (75 to 2.2 mg/L for C_4 to C_{10}) was modelled with very good agreement by Perturbed Chain Statistical Associating Fluid Theory (PC-SAFT), based on the extremely low vapor pressures for the $[C_nTHT][NTf_2]$-ILs measured in this work (4.15 to $0.037 \cdot 10^{-7} \times p_{sat}$ for C_4 to C_{10}). PC-SAFT is able to predict and correlate different thermodynamic properties by estimating the Helmholtz residual energy.

1. Introduction

Novel room temperature ionic liquids (RTILs) are attractive as a replacement for organic solvents due to their chemical and thermal stability, negligible vapor pressure, nonflammability as well as high ionic conductivity and wide electrochemical window.[1] The common ILs are pyridinium- and imidazolium-based ILs (Figure S1, SI).[2] Therefore, IL-cations with nitrogen atoms have been extensively investigated.[3,4,5,6,7]

Even if ILs are of interest for several decades by now, studies on sulfonium cations are not very advanced.[8,9,10] The first reported sulfonium-based ILs were trialkylsulfonium aluminum halides,[11] which are air and moisture sensitive. Matsumoto *et al.* described low viscosity, high conductivity and high electrochemical stability for symmetric trialkylsulfonium cations and various anions (for example bis(trifluoromethylsulfonyl) imide, $[NTf_2]^-$).[12,13] Orita *et al.* reported the physical properties of various sulfonium-, thiophenium- or thioxonium-based ILs (for the structure see Scheme 1) and their possible application as electric double-layer capacitors.[14]

In general, the resulting sulfonium salts are less stable than their imidazolium salts and therefore got less attention.[15] Zhang *et al.* reported some cyclic sulfonium RTILs (Scheme 1) which have decomposition temperatures between 272 and 285 °C, lower than for 1,3-dialkylimidazolium-based RTILs.[9] However, studies on cyclic sulfonium-based ILs are very rare, even if most of the developed cyclic sulfonium-based ILs exhibited strong hydrophilicity, restricting them to be used as electrolytes.[9] Guo *et al.* reported a novel family of hydrophobic cyclic sulfonium cations with $[NTf_2]^-$, which were applied in dye-sensitized solar cells.[16] However, their potential use as reaction media for the synthesis of nanomaterials is less explored.[17] Furthermore, due to the sulfur atom such sulfonium ILs have unique stabilizing abilities for bioenzymatic reactions. The sulfur moiety supports the enzymatic reactivity, leading to higher turnover rates in biocatalytic reactions.[18]

The solubility of ILs is a key factor for industrial application, e.g. for the utilization of ILs as additives to allow for larger hydrophobicity in aqueous solutions. IL application can thus allow for larger operating windows, effectively reducing consumption of energy and resources. The ability to incorporate solubility knowledge into process intensification or process

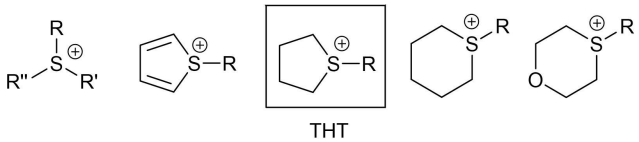

Scheme 1. (From left to right) Sulfonium, thiophenium, tetrahydrothiophenium (THT), cyclic sulfonium and thioxonium cations.

[a] Dr. A. Schmitz, D. Schmidt, F. Junglas, Dr. T.-O. Knedel, Prof. Dr. C. Janiak
Institut für Anorganische Chemie und Strukturchemie,
Heinrich-Heine-Universität Düsseldorf
40204 Düsseldorf (Germany)
E-mail: janiak@uni-duesseldorf.de
[b] M. Bülow, Dr. C. Held
Laboratory of Thermodynamics
Technische Universität Dortmund
44227 Dortmund (Germany)
[c] Dr. D. H. Zaitsau, Prof. Dr. S. P. Verevkin
Department of Physical Chemistry
University of Rostock
18059 Rostock (Germany)
[d] Dr. D. H. Zaitsau, Prof. Dr. S. P. Verevkin
Competence Centre CALOR
Faculty of Interdisciplinary Research
University of Rostock
18059 Rostock (Germany)

Supporting information for this article is available on the WWW under https://doi.org/10.1002/open.202000228

Special Issue *An invited contribution to a Special Issue dedicated to Material Synthesis in Ionic Liquids*

development through thermodynamic models gives way towards a greener chemistry. Thermodynamic models, like the here used Perturbed-Chain Statistical Associating Fluid Theory (PC-SAFT) equation of state,[19] are nowadays integrated as fundamentals in process simulation software.

PC-SAFT, able to predict and correlate various thermodynamic properties through estimating the residual Helmholtz energy, was already successfully applied to model solubilities in ternary mixtures of water, alcohol, and common imidazolium ILs.[20] Its electrolyte counterpart, ePC-SAFT,[21] was used to screen the solubility of the most common ILs and TAAILs (Tunable Aryl-Alkyl ILs) in binary and ternary aqueous systems.[22,23] Solubility predictions with ePC-SAFT was used to ensure interactions of TAAILs with various washing agents did not interfere the aggregation processes in catalytic nanoparticle synthesis.[24]

Aqueous solutions are still the primary reaction medium in the bio- and chemical industry. Thus, PC-SAFT is here again used to model the THT-IL solubility in water for future use in process intensification and development.

First of all, absolute vapor pressures are required as input for the PC-SAFT parameterization. However, these data are per se important for science and practical applications. One of the key advantages that are often highlighted for ILs is that they are considered non-volatile at ambient temperatures. However, as the temperature increases, the volatility of an IL also gradually increases. Consequently, at practically relevant and elevated temperatures typically used in industrial applications (e.g. for catalysis with Supported Ionic Liquid Phase (SILP)[25] and Supported Catalyst with Ionic Liquid Layer (SCILL))[26], the IL volatility could already be significant. The volatility is directly related to the vapor pressure. Hence, the vapor pressure of the IL at a certain temperature is therefore decisive for the IL mass loss from the catalyst. The comparison of the volatility of differently structured ILs enables an appropriate selection of suitable ILs for every practical purpose.

This work introduces S-alkyltetrahydrothiophenium, $[C_nTHT]^+$ bis(trifluorosulfonyl)imide, $[NTf_2]^-$ room temperature ionic liquids and tetraphenylborate, $[BPh_4]^-$ salts with alkyl chain lengths from C_4 to C_{10}. A detailed characterization was performed, including solid-state structures, density, viscosity and vapor pressure measurements. Additionally, PC-SAFT was applied to model the solubility in water for $[C_nTHT][NTf_2]$-ILs based on parametrization including the extremely low vapor pressures measured in this work.

2. Results and Discussion

2.1. Synthesis

Seven S-alkyl tetrahydrothiophenium bis(trifluoromethylsulfonyl)imide ILs, $[C_nTHT][NTf_2]$ and the corresponding tetraphenylborate salts, $[C_nTHT][BPh_4]$ were synthesized in two steps. The S-alkyl chains varied from n-butyl (C_4) to n-decyl (C_{10}) (Scheme 1). First, the $[C_nTHT]^+$ iodide intermediates were prepared from tetrahydrothiophene, THT and iodoalkanes, based on the synthesis of Zhang *et al.*[27] The second step involved the iodide anion exchange with either $Li[NTf_2]$ or $Na[BPh_4]$ (for further information see experimental section).

White crystalline products and yellow/orange oils were obtained for the S-alkyl tetrahydrothiophenium iodides, $[C_nTHT][I]$ salts in yields between 35% and 90% and verified by ^1H- and ^{13}C-nuclear magnetic resonance (NMR) as well as thermogravimetric analysis (TGA). The iodides still contained significant amounts of iodoalkane residues (by NMR, Figure S2–Figure S15), up to 40% for octyl/nonyl/decyl which could not be removed in high vacuum (10^{-7} mbar) for pentyl- or longer alkyl chains because of the high boiling points (157 °C for $C_5H_{11}I$ to 264 °C for $C_{10}H_{21}I$). The iodoalkanes could also not be removed from a solution of $[C_nTHT][I]$ in CH_2Cl_2 by extraction with heptane (as was successful for the purification of the $[C_nTHT][NTf_2]$-ILs (see below)).

The compound 1-nonyltetrahydrothiophenium iodide could be grown as colorless crystals from methanol. The molecular structure shows the nonyl group to be arranged in a straight, non-folded chain (Figure 1). The C-S-C angles at the pyramidal sulfur range from 94.1° in the ring to ~102° for C_{alkyl}-S-C_{ring}, the angle sum 298.3°. The crystal packing is dominated by the van der Waals interactions of the parallel-arranged nonyl chains together with the Coulomb interactions (Figure S54, SI). The shortest distance between sulfur and iodide is 3.66 Å. None of the other $[THT]^+$ iodides could be crystallized.

Subsequently, the iodide anion was exchanged with tetraphenylborate $[BPh_4]^-$ in ethanolic solution to improve the crystallization of the $[C_nTHT]^+$-cations. The tetraphenylborate salts were obtained in quantitative yield and verified by ^1H- and ^{13}C-NMR (Figure S16–Figure S29, SI), elemental analysis as well as thermogravimetric analysis (TGA). Calculated and found CHS values were in excellent agreement (Table S3, SI). The compounds $[C_nTHT][BPh_4]$ could be grown as colorless crystals from dichloromethane and ethanol for n = 4, 5 and 8 (Figure 2, Figure 3 and Figure 4).

The crystal packing in the compounds $[C_nTHT][BPh_4]$ is organized by Coulombic forces and CH-π interactions. There were no significant π-π-stacking interactions (Fig. S56-S58, SI).

In comparison to the corresponding S-alkyl tetrahydrothiophenium, $[C_nTHT]^+$ iodide and tetraphenylborate salts, the hydrophobic bis(trifluoromethylsulfonyl)imide, $[NTf_2]^-$ anion

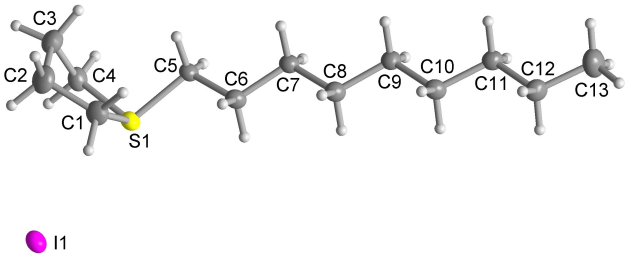

Figure 1. Molecular structure of an ion pair of 1-nonyltetrahydrothiophenium iodide, $[C_9THT]I$ (50% thermal ellipsoids). See Figure S54 (SI) for the packing diagram. Selected bond distances and angles are listed in Table S6, SI.

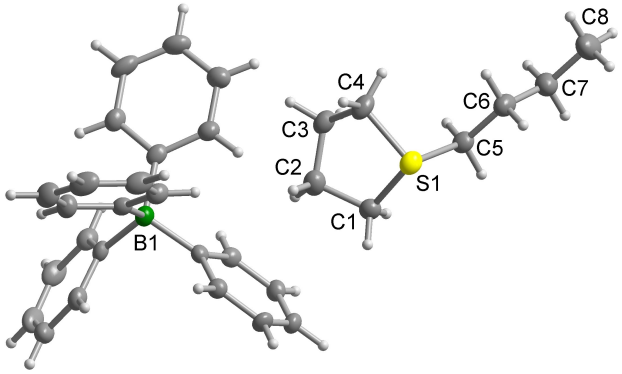

Figure 2. Molecular structure of one of the two symmetry-independent ion pairs in the asymmetric unit in the crystal structure of $[C_4THT][BPh_4]$ (50% thermal ellipsoids). Selected bond distances and angles are listed in Table S8, SI.

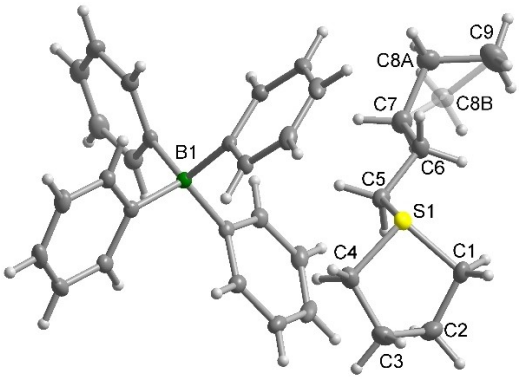

Figure 3. Molecular structure of one of the two symmetry-independent ion pairs in the asymmetric unit in the crystal structure of $[C_5THT][BPh_4]$ (50% thermal ellipsoids). A slight disorder for atom C8 A with 90% versus C8B with 10% occupancy is indicated. Selected bond distances and angles are listed in Table S9, SI.

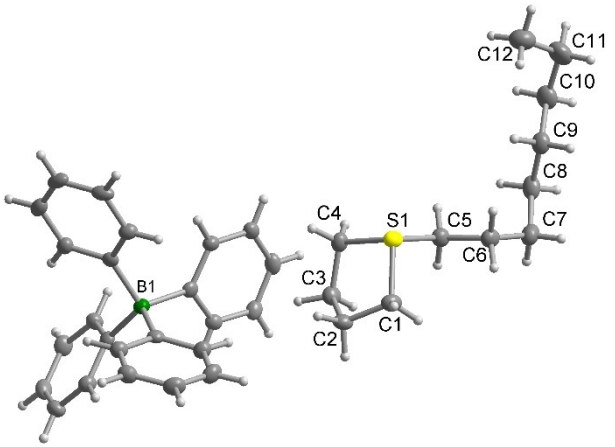

Figure 4. Molecular structure of an ion pair of $[C_8THT][BPh_4]$ (50% thermal ellipsoids). Selected bond distances and angles are listed in Table S10, SI.

renders the ion pairs as RTILs. These NTf_2-ILs were prepared by an I^- to $[NTf_2]^-$ anion exchange of $[C_nTHT]I$ with $Li[NTf_2]$ in an aqueous solution (Scheme 2). After anion exchange, the ILs

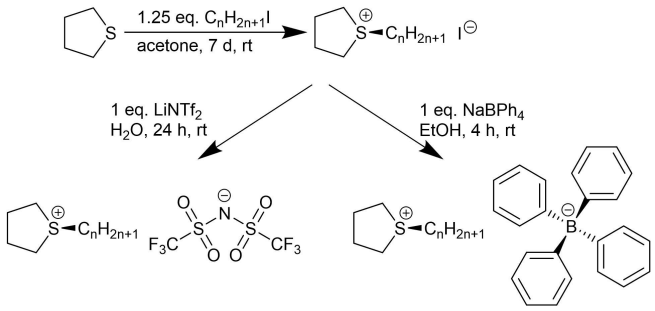

Scheme 2. Synthesis of S-alkyltetrahydrothiophenium bis (trifluoromethylsulfonyl)imide $[NTf_2]^-$-ILs and tetraphenylborate salts.

were extracted from the aqueous phase with dichloromethane and washed iodide-free with water and by stirring with activated charcoal. After filtration over acidic aluminum oxide, the ILs were extracted with heptane to remove iodoalkane impurities. In the ^{1}H-NMR spectra of $[C_nTHT][NTf_2]$ (Figure S30–Figure S43) no signals for iodoalkane impurities could be observed anymore. In the ^{13}C-NMR an additional quartet is observed at 119.7 ppm with $^1J_{C,F} = 321$ Hz for the CF_3 group in NTf_2^- (Figure S30–Figure S43).

The water content was measured by coulometric Karl-Fischer Titration for all ILs and was below 10 ppm, except for $[C_4THT][NTf_2]$ (< 100 ppm). All ILs were obtained with an anion purity of over 99% and an overall IL purity[24,28,29] of > 97%, typically > 99% (Table S1 and Figure S44–Figure S50). In addition, calculated and found CHNS elemental analysis values for $[C_4THT][NTf_2]$ were in very good agreement to each other (Table S4).

From thermogravimetric analyses (Figure S51–Figure S53) the $[C_nTHT]^+$ triflimide ILs exhibit the highest thermal stability of up to 270 °C, the iodides showed a decomposition temperature of 170 °C and tetraphenylborate salts had the lowest stability of only about 100 °C. (Table S2). In this work the thermal stability of an ionic liquid is defined as the ability of the material to resist thermal stress and to maintain its physical properties without degradation (decomposition). According to this definition, we studied the vapor pressure behavior of the series of ionic liquids in the as large as possible temperature range. This range is restricted by sensitivity of the quartz crystal microbalance (QCM) at low temperatures and by the thermal stability of the IL (i.e. the onset of decomposition) at elevated temperatures.

2.2. Ambient Pressure Liquid Density and Viscosity of $[C_nTHT][NTf_2]$-ILs

The temperature-dependent liquid density and viscosity are two important parameters for the design of processes. In the respective unit operations, the viscosity defines mass- and heat-transfer rates and influences the flow behaviour in tubing and reactors. For a possible application of ILs in the CO_2 separation, the viscosity is one of the most important physical properties. The dynamic viscosity of $[C_nTHT][NTf_2]$-ILs has been measured in

the temperature range of 293.15 to 323.15 K at ambient pressure, summarized in Table 1. The viscosity increases with increasing alkyl chain length and decreases with rising temperatures.

Likewise, the liquid density provides fundamentals in decision making for extraction and general application to processes. Furthermore, liquid densities give easy access to the parametrization procedure of thermodynamic models like equation of states. The liquid density of the $[C_nTHT][NTf_2]$-ILs was measured in the temperature range of 293.15 to 323.15 K at ambient pressure, summarized in Table 2. The liquid density decreases with increasing alkyl chain length of the $[C_nTHT][NTf_2]$-ILs. Likewise, the expectable temperature dependency for ILs with decreasing density at higher temperatures is valid for $[C_nTHT][NTf_2]$-ILs.

2.3. Absolute Vapor Pressures of ILs

Knowledge of vapor pressures is indispensable for practical applications of ILs, *e.g.* as thermofluids or catalysts. Vapor pressures of ILs measured in this work are significant for localization and optimization of the temperature for practical application of ILs, e.g. as a catalyst carrier. The vapor pressures of the ILs at the level of 10^{-3} Pa (even at elevated temperatures) are very good indicators that even in a flow chemical reactor the loss of the IL from the reactor can be considered as negligible (even at a large time scale). At the same time, it is meaningless to run the reactor at temperatures where thermal degradation could be possible. The TGA results do not reflect the actual processes occurring in the bulk IL, because the sample in the TGA crucible has a large surface/mass ratio, which is significantly different with those in QCM experiments and in a flow reactor. The frequency change rates ($df/d\tau$) measured by the quartz-crystal microbalance (QCM) were used for calculation of the absolute vapor pressures p_{sat} of ILs (see Table S14) with help of the empirical constant K' evaluated for our experimental setup recently.[30] The temperatures 373 K and 473 K seem to be of reasonable choice for many practical applications and extremely low values of vapor pressures of the $[C_nTHT][NTf_2]$-ILs at these temperatures (see Table 3, Figure 5) indicate that the negligible mass uptake of the IL in different catalytic or separation applications can be expected even at elevated temperatures.

Table 1. Measured dynamic viscosity of $[C_nTHT][NTf_2]$ ($n=4$–10) at ambient pressures for the temperature range of 293.15 to 323.15 K.

T [K]	Dynamic viscosity [mPa • s]						
	$[C_4]$	$[C_5]$	$[C_6]$	$[C_7]$	$[C_8]$	$[C_9]$	$[C_{10}]$
293.15	112.70	132.50	152.90	180.10	201.10	231.20	294.50
298.15	87.67	102.00	116.90	138.40	152.30	173.00	220.10
303.15	69.32	79.98	91.00	103.90	116.40	131.90	164.00
308.15	56.07	63.75	72.18	81.72	91.10	102.70	127.20
313.15	45.82	51.74	58.30	65.56	72.37	80.99	99.00
318.15	37.92	42.52	47.64	54.81	58.69	64.95	78.31
323.15	31.85	35.40	39.41	44.48	48.00	53.08	63.49

Table 2. Measured liquid density of $[C_nTHT][NTf_2]$ ($n=4$–10) at ambient pressures for the temperature range of 293.15 to 323.15 K.

T [K]	Liquid density [g • cm^{-3}]						
	$[C_4]$	$[C_5]$	$[C_6]$	$[C_7]$	$[C_8]$	$[C_9]$	$[C_{10}]$
293.15	1.4585	1.4311	1.3925	1.3700	1.3422	1.3163	1.2932
298.15	1.4536	1.4265	1.3878	1.3652	1.3369	1.3118	1.2885
303.15	1.4486	1.4218	1.3829	1.3630	1.3342	1.3072	1.2837
308.15	1.4436	1.4172	1.3780	1.3586	1.3298	1.3034	1.2787
313.15	1.4384	1.4127	1.3748	1.3541	1.3252	1.2987	1.2735
318.15	1.4359	1.4079	1.3692	1.3498	1.3206	1.2942	1.2691
323.15	1.4312	1.4033	1.3658	1.3432	1.3159	1.2904	1.2644

Table 3. Absolute vapor pressures of ionic liquids $[C_nTHT][NTf_2]$ at 373 K and at 473 K.

IL	$10^{-7}\times p_{sat}$, [Pa] 373 K	$10^{-3}\times p_{sat}$, [Pa] 473 K
$[C_4THT][NTf_2]$	4.15	558
$[C_5THT][NTf_2]$	2.59	560
$[C_6THT][NTf_2]$	1.82	633
$[C_7THT][NTf_2]$	1.0	742
$[C_8THT][NTf_2]$	0.39	608
$[C_9THT][NTf_2]$	0.23	627
$[C_{10}THT][NTf_2]$	0.037	244
$[(C_2H_5)_3S][NTf_2]$	52.5	881

2.4. Standard Molar Vaporization Enthalpies From Vapor Pressure Measurements

The standard molar enthalpies of vaporization derived from the temperature dependence of the vapor pressures measured with the QCM (see Table 4, column 5) are referenced to the average temperature T_{av} (see Table 4, column 4), which is the middle of the temperature range under study.

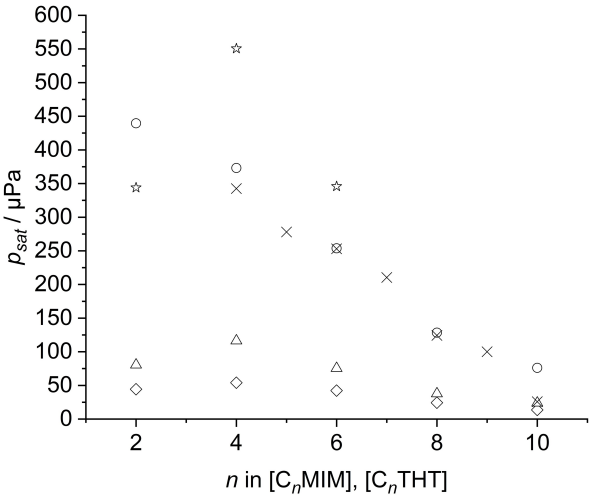

Figure 5. Chain-length dependence of absolute vapor pressures scaled with k at $T=423.15$ K for the homologous series $[C_nMIM][NTf_2]$ (○) from ref. [31] (k = 1/3), $[C_nMIM][PF_6]$ (◇) from ref. [30] (k = 3), $[C_nMIM][BF_4]$ (Δ) from ref. 30 (k = 3), $[C_nMIM][FAP]$ (☆) from ref. [32] (k = 1/3), $[C_nTHT][NTf_2]$ (x) this work (k = 1/3) (C_nMIM = 1-alkyl-3-methyl-imidazolium, FAP = tris(perfluoroalkyl) trifluoro-phosphate). For illustrative reason the absolute vapor pressures of ILs were scaled with the coefficients k given in parenthesis.

Table 4. Thermodynamics of vaporization of the [C_nTHT][NTf_2]-ILs derived from QCM measurements.

Cation	*T*-range K	T_{av}	$\Delta_l^g H_m^o(T_{av})$ kJ mol^{-1}	$\Delta_l^g G_m^o(T_{av})$[a]	$\Delta_l^g C_{p,m}^o$ [b] J·K^{-1} mol^{-1}	$\Delta_l^g H_m^o$(298.15 K)[c] kJ mol^{-1}
1	2		4	5	6	7
[C_4THT]	364-411	387.2	135.3 ± 1.0	76.6 ± 1.5	−86	143.0 ± 1.8
[C_5THT]	369-416	392.7	137.7 ± 1.0	76.0 ± 1.5	−94	146.6 ± 2.0
[C_6THT]]	369-419	393.5	140.6 ± 1.0	76.5 ± 1.5	−99	150.0 ± 2.1
[C_7THT]	369-423	394.8	143.4 ± 1.0	77.4 ± 1.5	−109	153.9 ± 2.3
[C_8THT]	374-423	398.5	146.4 ± 1.0	78.3 ± 1.5	−118	158.2 ± 2.6
[C_9THT]	374-424	399.1	149.5 ± 1.0	79.2 ± 1.5	−124	162.0 ± 2.7
[C_{10}THT]	382-431	406.0	153.8 ± 1.0	81.4 ± 1.5	−134	168.2 ± 3.1
[$(C_2H_5)_3S$]	357-405	380.1	120.6 ± 1.0	71.5 ± 1.5	−70	126.4 ± 1.5

[a] The standard Gibbs energies of vaporization were evaluated using the calibration coefficient developed in our recent work.[30] [b] From Table S15. [c] Adjusted to 298.15 K using the $^g_l C^o_{p,m}$-values from column 6. Uncertainties in the temperature adjustment of vaporization enthalpies from T_{av} to the reference temperature are estimated to account with 20% to the total adjustment.

Absolute vapor pressures and vaporization enthalpies of the [C_nTHT][NTf_2]-ILs have been measured for the first time. According to thermochemical praxis, the measured enthalpies of vaporization $\Delta_l^g H_m^o(T_{av})$ have to be adjusted to the reference temperature 298.15 K, for the sake of the understanding of the structure-property relations. The vaporization enthalpy $\Delta_l^g H_m^o$(298.15 K) at the reference temperature is calculated according to Eq. 7. The $\Delta_l^g C_{p,m}^o$-values were calculated with an empirical equation:[31]

$$\Delta_l^g C_{p,m}^o = C_{pm}^o(l,\ 298.15\,\mathrm{K})\ (-0.26 \pm 0.05) + (68.7 \pm 37.0) \quad (1)$$

which is based on the experimental data on C_{pm}^o(l, 298.15 K) of the [C_nTHT][NTf_2]. The C_{pm}^o (*l*, 298.15 K) and the $\Delta_l^g C_{p,m}^o$-values required for the temperature adjustments of vaporization enthalpies according to Eq. 1 are compiled in Table S15.

2.5. Chain Length Dependence of Vaporization Enthalpies

A monotonic increase of vaporization enthalpies in a homologous series with the growing chain length is well-established phenomena. This behaviour is common for molecular as well as for ionic compounds.[31] For example, the $\Delta_l^g H_m^o$(298.15 K)-values in a homologous series of imidazolium based ionic liquids [C_nMIM][NTf_2] increases with the number of carbon atoms, (N_C), in the alkyl chain (from 2 to 18) according to Eq. 2:[31]

$$\Delta_l^g H_m^o(298.15\,\mathrm{K})/\mathrm{kJ}\cdot\mathrm{mol}^{-1} = 3.9 \times (N_C) + 115.7\ (\text{with } R^2 = 0.999) \quad (2)$$

The enthalpy of vaporization in the homologous series [C_nTHT][NTf_2] studied in this work also correlates linearly with the chain length as follows:

$$\Delta_l^g H_m^o(298.15\,\mathrm{K})/\mathrm{kJ}\cdot\mathrm{mol}^{-1} = 4.1 \times (N_C) + 125.9\ (\text{with } R^2 = 0.992) \quad (3)$$

The linear trends have been also observed (see Table S16) for the imidazolium-based ILs with the fluorinated cations $[NTf_2]^-$, $[PF_6]^-$, $[BF_4]^-$, $[FAP]^-$. It is apparent from Table S16 that slopes of all considered linear dependencies are very close and they are generally representing the very similar "additive" contribution of the CH_2-group to the vaporization enthalpy $\Delta_l^g H_m^o$(298.15 K) independent on the structure of the IL-cation and IL-anion. This observation indicates the general consistency of the experimental data on vaporization enthalpies measured in this work.

2.6. Comparison of Vaporization Enthalpies of Cyclic and Non-Cyclic Ionic and Molecular Compounds

Structure-property relationships is important quantitative and qualitative way to rationalize experimental results. Indeed, in the frame of this work we studied ionic liquids with the cyclic S-containing cations of general formula $[C_n THT]^+$, as well as the ionic liquid with non-cyclic cation $[(C_2H_5)_3S]^+$. It is interesting now to reveal an impact of cyclisation on the vaporization enthalpy. For this purpose we need to compare enthalpy vaporization of [$(C_2H_5)_3S$][NTf_2] with those of [C_2THT][NTf_2] which has the same molecular formula. The latter value $\Delta_l^g H_m^o$(298.15 K, [C_2THT][NTf_2]) = 134.1 ± 3.5 kJ·mol^{-1} was calculated according to Eq. 3. This value is somewhat larger in comparison to the value $\Delta_l^g H_m^o$(298.15 K, [$(C_2H_5)_3S$][NTf_2]) = 126.4 ± 1.5 kJ·mol^{-1} (see Table 2). It is apparent, that cyclisation of the IL-cation in *ionic compounds* increases vaporization enthalpy, because the cyclic molecules are arranged in the liquid phase more compact in comparison to the branched $[(C_2H_5)_3S]^+$ cation. Is this trend the same in molecular compounds? Let us compare enthalpy vaporization of the cyclic amine N-ethyl-pyrrolidine ($\Delta_l^g H_m^o$(298.15 K) = 37.4 ± 0.7 kJ·mol^{-1}[33]) with those of open-chained tri-ethylamine ($(C_2H_5)_3N$ ($\Delta_l^g H_m^o$(298.15 K) = 35.0 ± 0.2 kJ·mol^{-1}[34]) which has the same molecular formula. The value for the cyclic *molecular compound* is somewhat larger in comparison to those for open-chained branched compound. Thus, the regularities observed for the *ionic* and for the *molecular* compounds have shown the same trend. This observation again indicates the general consistency of the experimental data on vaporization enthalpies measured in this work.

2.7. PC-SAFT Parametrization of $[C_nTHT][NTf_2]$-ILs Using Vapor Pressure and Liquid Density

Thermodynamic models are nowadays important tools for process development, optimization and controlling, such as Perturbed-Chain Statistical Associating Fluid Theory (PC-SAFT). Providing the necessary inputs for the here synthesized $[C_nTHT][NTf_2]$-ILs, pure-component parameters for PC-SAFT have been regressed. PC-SAFT is a vital thermodynamic model for predicting and correlating process properties, including e.g. liquid-liquid equilibria. The pure-component parameters are a physically meaningful abstraction of the actual molecule ($[C_nTHT][NTf_2]$-IL). In total, five pure-component parameters for each $[C_nTHT][NTf_2]$-IL are fitted directly to the measured pure liquid density and the extremely low vapor pressures. This fitting routine is a new development[35] accessing the unbiased modelling of thermodynamic properties for electrolytes. Handling the very low vapor pressure of $[C_nTHT][NTf_2]$-ILs is numerically challenging and needs a sophisticated algorithm. Computational details on PC-SAFT modelling are listed in the SI. The pure-component parameters for the $[C_nTHT][NTf_2]$-ILs are summarized in Table 5. Following previous publications on IL parametrization with electrolyte PC-SAFT,[36,37] a linear dependency with the chain length of the $[C_nTHT][NTf_2]$-ILs, and thus molecular weight, as depicted by both vapor pressure and liquid density was also assumed for the pure-component parameters of the $[C_nTHT][NTf_2]$-ILs. Figure 6 exemplarily shows the results of the parameter estimation for $[C_{10}THT][NTf_2]$. Linear equations for the pure-component parameters are listed in the SI.

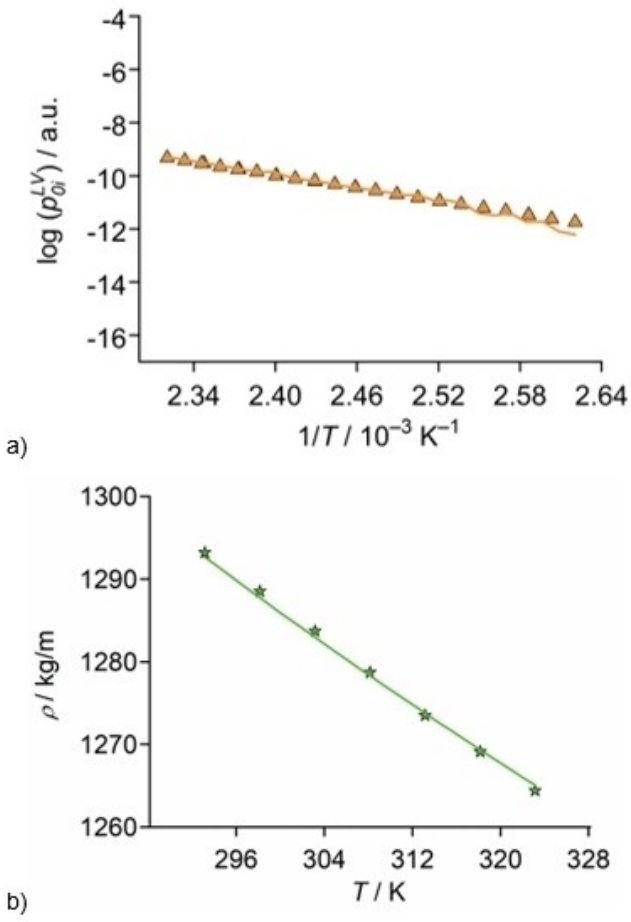

Figure 6. (a) PC-SAFT modelled and experimental vapor pressure for $[C_{10}THT][NTf_2]$. (b) PC-SAFT modelled and experimental liquid density for $[C_{10}THT][NTf_2]$ at ambient pressure.

2.8. Solubility of ILs

For the use of ILs in aqueous-based applications (*e.g.* extraction of impurities or as co-solvent in enzymatic reactions) it is important to know their solubility in water. Because these mostly take place in aqueous solutions in which the IL should only be used as an additive. For the solubility three solution of each ionic liquid were prepared above the solubility limit. The content of the IL in the aqueous phase was then determined by ion chromatography, after the solutions was stirred for seven days so that both phases are in an equilibrium. The results are shown in Figure 7.

2.9. Modelling the Solubility of $[C_nTHT][NTf_2]$-ILs in Water with PC-SAFT

The solubility of $[C_nTHT][NTf_2]$-ILs in water is a key property for the application in chemical and biochemical processes. $[C_nTHT][NTf_2]$-ILs are superior additives in enzymatic reactions[38] and can be used to widen the solubility of hydrophobic compounds. PC-SAFT is used to model the solubility of the $[C_nTHT][NTf_2]$-ILs in water for 298.15 K, giving easy access to further applications of the $[C_nTHT][NTf_2]$-ILs. The experimental

Table 5. PC-SAFT pure-component parameters for the $[C_nTHT][NTf_2]$-ILs.[a]

Pure-component parameters	$[C_4THT]$ [NTf2]	$[C_5THT]$ [NTf2]	$[C_6THT]$ [NTf2]	$[C_7THT]$ [NTf2]	$[C_8THT]$ [NTf2]	$[C_9THT]$ [NTf2]	$[C_{10}THT]$ [NTf2]
Molar Mass [g/mol]	425.4	439.5	453.5	467.5	481.5	495.6	509.6
σ_i [A]	5.70	5.65	5.60	5.55	5.51	5.46	5.41
m_{seg}	2.67	2.93	3.18	3.44	3.69	3.94	4.20
u_i/kB [K]	752.14	723.12	694.23	665.33	636.44	607.34	578.44
ε^{AiBi}/kB [K]	2412.92	2577.15	2740.67	2904.20	3067.73	3232.42	3395.95
κ^{AiBi}	0.051	0.044	0.037	0.031	0.024	0.017	0.010

[a] 2B association scheme, see Supp. Info. Table S18 and S19.

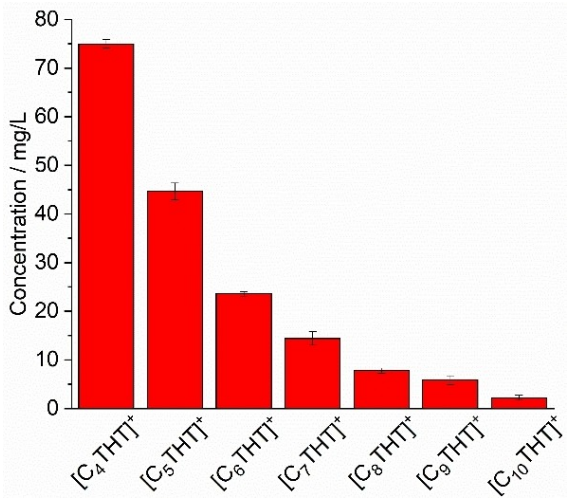

Figure 7. Solubility of the seven ILs in water at room temperature and ambient pressure.

data is summarized in Table S20 in the SI. The modelling results are presented in Figure 8 and are in good agreement with the experimental data. Using the very small vapor pressures of $[C_n THT][NTf_2]$-ILs in the parametrization is complex, however, gives advantages in the modelling process.

3. Conclusions

This work describes the synthesis of seven RTILs $[C_n THT][NTf_2]$ starting from tetrahydrothiophene (THT) with the addition of the respective alkyl iodide $C_nH_{2n+1}I$. From the intermediate S-alkyl tetrahydropthiophenium iodides, $[C_n THT]I$ the salt-metathesis iodide anion exchange with $Li[NTf_2]$ or $Na[BPh_4]$ delivered the bis(trifluoromethylsulfonyl)imide ILs and the tetraphenylborate $[C_n THT][BPh_4]$ salts. For the latter, three examples (C_4, C_5 and C_8) could be structurally elucidated by single-crystal X-ray crystallography, showing CH-π packing interactions together with the Coulomb forces.

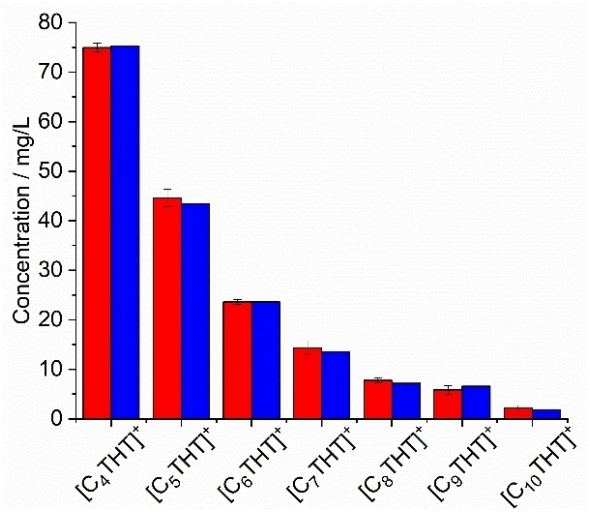

Figure 8. Experimental and modelled solubility of $[C_n THT][NTf_2]$-ILs in water at 298.15 K and 1 bar. PC-SAFT pure-component parameters and binary interaction parameters listed in Table 5 and Table S20.

The RTILs could be obtained as pure compounds with water contents below 10 ppm (except C_4 below 100 ppm) and an anion purity of 99%. Viscosities, liquid densities and vapor pressures were determined experimentally and modelled with PC-SAFT. Viscosities and densities decreased with increasing temperature. Additionally, the viscosities increased with longer alkyl chains whereas the densities decreased with the alkyl chain length. The vapor pressures for the ILs were very small even at higher temperatures. Finally, the solubility of the ILs in water could be successfully modelled with PC-SAFT and verified/measured by ion chromatography. Solubility is as a key property for potential applications of IL in aqueous systems, e.g. for the utilization of ILs as additives to provide for larger hydrophobicity in aqueous solutions.

Experimental Section

General

All synthetic experiments were carried out under nitrogen or argon using Schlenk techniques, since the iodide ILs are hygroscopic. Just the anion exchanges were carried out under air atmosphere. All products were stored in a glovebox (mBraun Labmaster 130) under argon atmosphere. 1-iodobutane (99%), 1-iodoheptane (98%), 1-iododecane (98%) and tetrahydrothiophene (99%) were purchased from Sigma Aldrich, 1-iodooctane (98%) and 1-iodohexane (98%) from Acros Organics, 1-iodopentane (98%) from Alfa Aesar, 1-iodononane (98%) from TCI and sodium tetraphenylborate (99.5%) from Merck. Lithium bis(trifluoromethylsulfonyl)imide was obtained from J&K. All chemicals were used without further purification. The sample of $[(C_2H_5)_3S][NTf_2]$ was of commercial origin (Iolitech GmbH).

Instrumentation

Coulometric Karl Fischer titration was performed with an ECH/Analytik Jena AQUA 40.00 Karl Fischer titrator. The measurements were done with the headspace module with dried sample container and crimp caps (Ø = 20 mm, with PTFE septum). The measurements were done at a temperature of 170 °C.

Thermogravimetric analysis (TGA) was carried out with a Netzsch TG 209 F3 Tarsus, equipped with Al-crucible using a heating rate of 5 K min^{-1} under inert atmosphere (N_2) between 30 °C and 600 °C. The TGA studies have been used in this work as an auxiliary method in order to only assess the highest possible temperature for the QCM experiment below the decomposition temperature of the IL. The mass-loss (decomposition or evaporation) temperatures in the TGA were determined by the onset value which in turn was derived from the intersection of the two tangents placed at the mass-temperature curve.

The melting points were measured on a Melting Point B-540 from Büchi.

Ion chromatographic measurements (IC) were carried out using a Dionex ICS 1100 instrument with suppressed conductivity detection. The system was equipped with the analytical column IonPac AS 22 from Dionex (4×250 mm) with the corresponding guard column AG 22 (4×50 mm), respectively. The suppressor (AERS 500, Dionex) was regenerated with an external water module. The

instrument was controlled by Chromeleon® software (version 7.1.0.898). The injection volume was 25 μL. To the standard eluent (4.5 mmol L^{-1} Na_2CO_3 + 1.0 mmol L^{-1} $NaHCO_3$) 30 vol.–% acetonitrile was mixed.

IR-spectra were recorded on a Bruker Tensor 37 IR with ATR unit in the range of 4000–600 cm^{-1}.

^{1}H- and ^{13}C-NMR spectra were measured on a Bruker Avance III-600, an Avance III-300 or an Avance DRX 500 NMR-spectrometer at 298 K. The H,H coupling constants are reported as absolute values. The assignment of the $[THT]^+$ resonances was confirmed by 2D techniques and is consistent with earlier studies by Wenzel and Cameron.[39]

The elemental analyses were measured at a Perkin Elementar Vario EL III analyzer.

The single-crystal X-ray structure data were collected on a Bruker Kappa Duo APEX-II with CCD area-detector, Mo-$K\alpha$ radiation (λ = 0.71073 Å), microfocus tube, multilayer mirror, ω and φ-scan scan; data collection with Apex2,[40] cell refinement and data reduction with SAINT, experimental absorption correction with SADABS.[41] Structure solution by direct methods using SHELXS-2018; refinement by full-matrix least squares on F^2 using the SHELXL-2018 program suite.[42,43] All non-hydrogen positions were refined with anisotropic displacement parameters. Hydrogen atoms on carbon atoms were positioned geometrically (with, C–H = 0.98 Å for CH_3, and C–H = 0.99 for CH_2) and refined using riding models (AFIX 137 and 23, respectively) with $U_{iso}(H) = 1.2U_{eq}(C)$ and $U_{iso}(H) = 1.5U_{eq}(C)$. Graphics were drawn with DIAMOND (Version 4).[44]

Measurements of Vaporization Enthalpies by the Quartz Crystalline Microbalance (QCM)

Heat Capacity Measurements

Isobaric heat capacities of liquid samples of $[C_nTHT][NTf_2]$ ionic liquids were determined by use of a heat-compensation technique in the Perkin Elmer Pyrus DSC 1 over the temperature range from 310 K to 376 K. The temperature calibration of the DSC was conducted with highly pure (> 99.9 mas%) reference materials indium, tin and lead. Temperature was measured with the standard uncertainty of 0.2 K. Standard calorimetric pans and samples (around 10 to 15 mg) were weighted with a Sartorius MSE3.6P-000-DM microbalance with the standard uncertainty of $5 \cdot 10^{-6}$ g.

The heat capacity measurements were carried in three steps. The first thermal scan was performed for an empty pan. In the second thermal scan the reference material (sapphire) was measured. The third run was carried out with the sample of the ionic liquid.

According to and elaborated by the Perkin Elmer procedure, the whole temperature range of the typical DSC run was split in intervals of 50 K. The thermal profile of each interval started with a 2 min isothermal step followed with a temperature rise of 50 K (with a heating rate of 10 K·min^{-1}) and finished with an isothermal step over a 2 min period at the final temperature. The whole measuring profile was repeated four times and the results were averaged. The heat capacity was evaluated with the Perkin Elmer software.

The procedure of the heat capacity determination was tested with measurements on the reference sample of benzoic acid. The expanded uncertainty (k = 2) for the heat capacity measured by this method for ILs was estimated to be $0.02 \times C^{\circ}_{p,m}(\text{liq},\ 298\ \text{K})$.

Before beginning the heat capacity measurements, the IL samples were kept at 333 K and 10^{-5} Pa for 1 hour to remove possible traces of moisture and residual solvents.

The absolute vapor pressures and the standard molar enthalpies of vaporization of the S-ILs series were determined by using the QCM method.[45] The vaporization enthalpies were derived from the temperature dependencies of the experimentally measured change in the vibrational frequency of the quartz crystal. In the QCM method a sample of an IL is placed in an open cavity (Langmuir evaporation) inside of the thermostatted block and it is exposed to vacuum (10^{-5} Pa) with the whole open surface of the loaded compound. The QCM sensor is placed directly above the measuring cavity containing the sample. During the vaporization into vacuum, a certain amount of sample is deposited on the quartz crystal. The change of the vibrational frequency Δf was directly related to the mass deposition Δm on the crystal according to the Sauerbrey equation:[46]

$$\Delta f = -C \cdot f^2 \cdot \Delta m \cdot S_C^{-1} \tag{4}$$

where f is the fundamental frequency of the crystal (6 MHz in this case) with $\Delta f \ll f$, S_C is the surface of the crystal, and C is a constant.[30] The measured frequency change rates ($df/d\tau$) can be used for calculation of absolute vapor pressures p_s according to equation:

$$p_s = K' \frac{df}{dt} \sqrt{\frac{T}{M}}. \tag{5}$$

where the $K' = (9.5 \pm 1.1) \cdot 10^{-6}$ Pa·s·$kg^{1/2}$·Hz^{-1}·$K^{-1/2}$·$mol^{-1/2}$ is the empirical constant containing all parameters of the Sauerbrey equation as well as parameters specific for the geometry of the experimental setup.[30] The K'-value for our apparatus was evaluated with the help of reliable vapor pressure data on imidazolium and pyridinium based ILs compiled in references 30. Using the experimental vapor pressures p_s measured with the QCM technique the molar enthalpy of vaporization, $\Delta_l^g H^{\circ}_m(T)$ at experimental temperatures is obtained according to the Clarke-Glew equation:[47]

$$R\ln(p_s/p^{\circ}) = -\frac{\Delta_l^g G^{\circ}_m(T_{av})}{T_{av}} + \Delta_l^g H^{\circ}_m(T_{av})\left(\frac{1}{T_{av}} - \frac{1}{T}\right) + \Delta_l^g C^{\circ}_{p,m}\left(\frac{T_{av}}{T} - 1 + \ln\left(\frac{T}{T_{av}}\right)\right) \tag{6},$$

where T_{av} is the average temperature interval of the study. The value $\Delta_l^g C^{\circ}_{p,m} = C^{\circ}_{p,m}(g) - C^{\circ}_{p,m}(liq)$ is the difference between the molar heat capacities of the gaseous, $C^{\circ}_{p,m}(g)$, and the liquid phase, $C^{\circ}_{p,m}(liq)$, respectively. The vaporization enthalpy $\Delta_l^g H^{\circ}_m(298.15\ K)$ at the reference temperature is calculated according to the Kirchhoff's equation:

$$\Delta_l^g H^{\circ}_m(298.15\ K) = \Delta_l^g H^{\circ}_m(T_{av}) + \Delta_l^g C^{\circ}_{p,m}(298.15 - T_{av}) \tag{7},$$

where T_{av} is the average temperature of the temperature range of the QCM study. In order to detect and avoid any possible effect of impurities on the measured frequency loss rate ($df/d\tau$), a typical experiment was performed in a few consequent series with increasing and decreasing temperature steps. Every series consisted of 7 to 11 temperature points of mass loss rate determination. Several runs have been performed to test the reproducibility of the results. The study was finished when the enthalpy of vaporization,

$\Delta_l^g H_m^o$(298.15 K), obtained in the sequential runs by adjusting Eq. 7 to the temperature dependent rates (df/dτ) agreed within the assessed experimental uncertainty of about ± 1 kJ·mol^{-1}. In order to confirm the absence of decomposition of IL under the experimental conditions, the residual IL in the crucible and the IL-deposit on QCM were analyzed by ATR-IR spectroscopy. As can be seen in Figure S59 of the Supporting Information no changes in the spectra have been detected for ILs under study. Primary experimental results of the QCM studies are given in Table S14 in the Supporting Information. The final uncertainty of the absolute vapor pressure determination is estimated to be 50% and mostly determined by the uncertainty of K' coefficient.

General Synthesis of Tetrahydrothiophene Ionic Liquids

The synthesis of ILs was a two-step synthesis consisting of alkylation of the tetrahydrothiophene and anion exchange with Li[NTf_2] or Na[BPh_4] (Scheme 2). In the first step, the tetrahydrothiophene was dissolved in dry acetone and 1.25 eq. of the iodoalkane was added. After seven days in the dark the solvent was removed under reduced pressure and the IL was recrystallized several times in diethyl ether. For the anion exchange, the IL was dissolved in water and 1 eq. of lithium bis(trifluoromethylsulfonyl)imide was added. The two-phase system was stirred for 24 h at room temperature. The organic phase was extracted two times with dichloromethane and washed with water until the aqueous phase is iodide free. Then the IL was washed with hexane three times. The solvent was removed in vacuum and the IL was dried in vacuum at 80 °C for several hours. The IL was obtained as colorless liquid. For further characterization and for the NMR spectra see Supporting Information.

1-Butyltetrahydrothiophenium Iodide: The product was obtained as a white solid (54.6 g, 89%). ^{1}H-NMR ($CDCl_3$, 300 MHz, 298 K): δ 0.95 (t, $^3J_{HH}$ = 7.3 Hz, CH_3, 3H); 1.53 (h, $^3J_{HH}$ = 7.4 Hz, CH_2, 2H); 1.78 (q, $^3J_{HH}$ = 7.55 Hz CH_2, 2H); 2.42–2.50 (m, $(CH_2)_2$, 4H); 3.52 (t, $^3J_{HH}$ = 7.5 Hz, CH_2, 2H); 3.56–3.67 (m, $(CH)_2$, 2H); 3.76–3.92 (m, $(CH)_2$, 2H). ^{13}C-NMR ($CDCl_3$, 75 MHz, 298 K): δ 13.64 (CH_3); 21.52 (CH_2); 27.44 (CH_2); 29.15 (($CH_2)_2$); 42.27 (CH_2); 44.35 (($CH_2)_2$). TGA (5 K·min^{-1}): decomp. (T_{onset}): 123 °C.

1-Pentyltetrahydrothiophenium Iodide: The product was obtained as a light-yellow oil (50.4 g, 86%). ^{1}H-NMR ($CDCl_3$, 300 MHz, 298 K): δ 0.37 (t, $^3J_{HH}$ = 7.2 Hz, CH_3, 3H); 0.81–0.99 (m, $(CH_2)_2$, 4H); 1.29 (q, $^3J_{HH}$ = 7.5 Hz, CH_2, 2H); 1.92–2.03 (m, $(CH_2)_2$, 4H); 3.08 (t, $^3J_{HH}$ = 7.6 Hz, CH_2, 2H); 3.62–3.69 (m, $(CH)_2$, 2H); 3.81–3.93 (m, $(CH)_2$, 2H). ^{13}C-NMR ($CDCl_3$, 75 MHz, 298 K): δ 12.32 (CH_3); 20.56 (CH_2); 23.68 (CH_2); 27.64 (CH_2); 28.56 (($CH_2)_2$); 40.68 (CH_2); 42.70 (($CH_2)_2$). TGA (5 K·min^{-1}): decomp. (T_{onset}): 118 °C.

1-Hexyltetrahydrothiophenium Iodide: The product was obtained as a light orange oil (52.6 g, 90%). ^{1}H-NMR ($CDCl_3$, 600 MHz, 298 K): δ 0.78 (t, $^3J_{HH}$ = 7.0 Hz, CH_3, 3H); 1.19–1.23 (m,($CH_2)_2$, 4H); 1.42 (p, $^3J_{HH}$ = 7.4 Hz, CH_2, 2H); 1.71 (p, $^3J_{HH}$ = 7.7 Hz, CH_2, 2H); 2.37–2.47 (m, $(CH_2)_2$, 4H); 3.49 (t, $^3J_{HH}$ = 7.8 Hz, CH_2, 2H); 3.55–3.62 (m, $(CH)_2$, 2H); 3.78–3.85 (m, $(CH)_2$, 2H). ^{13}C-NMR ($CDCl_3$, 150 MHz, 298 K): δ 12.30 (CH_3); 20.51 (CH_2); 23.77 (CH_2); 26.02 (CH_2); 27.47 (–CH_2); 29.32 (($CH_2)_2$); 40.49 (CH_2); 42.53 (($CH_2)_2$). TGA (5 K·min^{-1}): decomp. (T_{onset}): 116 °C.

1-Heptyltetrahydrothiophenium Iodide: The product was obtained as a light-yellow oil (18.66 g, 65%). ^{1}H-NMR ($CDCl_3$, 300 MHz, 298 K): δ 0.82 (t, $^3J_{HH}$ = 6.9 Hz, CH_3, 3H); 1.20–1.31 (m, $(CH_2)_4$, 6H); 1.46 (p, $^3J_{HH}$ = 7.4 Hz, CH_2, 2H); 1.76 (p, $^3J_{HH}$ = 7.7 Hz, CH_2, 2H); 2.41–2.50 (m, $(CH_2)_2$, 4H); 3.52 (t, $^3J_{HH}$ = 7.7 Hz, CH_2, 2H); 3.56–3.65 (m, $(CH)_2$, 2H); 3.81–3.90 (m, $(CH)_2$, 2H). ^{13}C-NMR ($CDCl_3$, 75 MHz, 298 K): δ 13.46 (CH_3); 21.87 (CH_2); 25.01 (CH_2); 27.55 (CH_2); 28.10 (CH_2); 28.62 (CH_2); 30.79 (($CH_2)_2$); 41.83 (CH_2); 43.74 (($CH_2)_2$). TGA (5 K·min^{-1}): decomp. (T_{onset}): 115 °C.

1-Octyltetrahydrothiophenium Iodide: The product was obtained as a light-yellow oil (22.79 g, 44%). ^{1}H-NMR ($CDCl_3$, 300 MHz, 298 K): δ 0.82 (t, $^3J_{HH}$ = 5.7 Hz, CH_3, 3H); 1.21–1.50 (m, $(CH_2)_5$, 10H); 1.76 (p, $^3J_{HH}$ = 7.3 Hz, CH_2, 2H); 2.42–2.52 (m, $(CH_2)_2$, 4H); 3.53 (t, $^3J_{HH}$ = 7.5 Hz, CH_2, 2H); 3.57–3.68 (m, $(CH)_2$, 2H); 3.81–3.93 (m, $(CH)_2$, 2H). ^{13}C-NMR ($CDCl_3$, 75 MHz, 298 K): δ 14.04 (CH_3); 22.53 (CH_2); 25.59 (CH_2); 28.23 (CH_2); 29.13 (CH_2); 30.45 (CH_2); 31.61 (CH_2); 33.51 (($CH_2)_2$); 42.59 (CH_2); 44.37 (($CH_2)_2$). TGA (5 K·min^{-1}): decomp. (T_{onset}): 106 °C.

1-Nonyltetrahydrothiophenium Iodide: The product was obtained as a light-yellow oil (43 g, 81%). ^{1}H-NMR ($CDCl_3$, 500 MHz, 298 K): δ 0.66 (t, $^3J_{HH}$ = 6.8 Hz, CH_3, 3H); 1.05–1.15 (m, $(CH_2)_6$, 12H); 1.31 (p, $^3J_{HH}$ = 7.3 Hz, CH_2, 2H); 1.61 (p, $^3J_{HH}$ = 7.6 Hz, CH_2, 2H); 2.27–2.36 (m, $(CH_2)_2$, 4H); 3.41 (t, $^3J_{HH}$ = 8.2 Hz, CH_2, 2H); 3.47–3.55 (m, $(CH)_2$, 2H); 3.66–3.76 (m, $(CH)_2$, 2H). ^{13}C-NMR ($CDCl_3$, 125 MHz, 298 K): δ 13.57 (CH_3); 22.08 (CH_2); 25.18 (CH_2); 27.75 (CH_2); 28.61 (CH_2); 28.73 (CH_2); 29.96 (CH_2); 31.25 (CH_2); 33.06 (($CH_2)_2$); 42.06 (CH_2), 43.94 (($CH_2)_2$). TGA (5 K·min^{-1}): decomp. (T_{onset}): 148 °C.

1-Decyltetrahydrothiophenium Iodide: The product was obtained as a light-yellow oil (18.28 g, 38%). ^{1}H-NMR ($CDCl_3$, 500 MHz, 298 K): δ 0.78 (t, $^3J_{HH}$ = 6.8 Hz, CH_3, 3H); 0.98–1.33 (m, $(CH_2)_7$, 14H); 1.42 (p, $^3J_{HH}$ = 8.4 Hz, CH_2, 2H); 1.71 (p, $^3J_{HH}$ = 7.4 Hz, –CH_2, 2H); 2.19–2.41 (m, $(CH_2)_2$, 4H); 3.51 (t, $^3J_{HH}$ = 8.15 Hz, CH_2, 2H); 3.56–3.65 (m, $(CH)_2$, 2H); 3.78–3.89 (m, $(CH)_2$, 2H). ^{13}C-NMR ($CDCl_3$, 125 MHz, 298 K): δ 13.92 (CH_3); 22.47 (CH_2); 25.53 (CH_2); 28.13 (CH_2); 28.36 (CH_2); 29.05 (CH_2); 29.29 (CH_2); 30.33 (CH_2); 31.66 (CH_2); 33.43 (($CH_2)_2$); 42.49 (CH_2); 44.32 (($CH_2)_2$). TGA (5 K·min^{-1}): decomp. (T_{onset}): 166 °C

1-Butyltetrahydrothiophenium Tetraphenylborate: The product was obtained as a white solid (0.79 g, 93%). ^{1}H–NMR: (500 MHz, CD_3CN, 298 K): δ 0.95 (t, $^3J_{HH}$ = 7.35 Hz, CH_3, 3H); 1.46 (h, $^3J_{HH}$ = 7.4 Hz, CH_2, 2H); 1.75 (p, $^3J_{HH}$ = 7.6 Hz, CH_2, 2H); 2.13–2.29 (m, $(CH_2)_2$, 4H); 3.01 (t, $^3J_{HH}$ = 7.6 Hz, CH_2, 2H); 3.17–3.26 (m, $(CH)_2$, 2H); 3.36–3.46 (m, $(CH)_2$, 2H); 6.85 (t, $^3J_{HH}$ = 7.2 Hz, $(CH)_{para}$, 4H); 7.00 (t, $^3J_{HH}$ = 7.5 Hz, $(CH)_{meta}$, 8H); 7.22-7.34 (m, $(CH)_{ortho}$, 8H). ^{13}C-NMR: (125 MHz, CD_3CN, 298 K): δ 13.60 (CH_3); 22.11 (CH_2); 27.72 (CH_2); 29.27 (CH_2); 42.72 (CH_2); 44.18 (($CH_2)_2$); 122.80 (C_{para}); 126.58 (C_{meta}); 136.80 (C_{ortho}); 164.66 (^{1}JCB = 49 Hz, C_{ipso}). Elemental analysis [%] calc. for $C_{32}H_{37}SB$: C: 82.74%, H: 8.03%, S: 6.90%; Found: C: 83.01%, H: 7.58%, S: 6.94%. Melting point: 180 °C TGA (5 K·min^{-1}): decomp. (T_{onset}): 234 °C.

1-Pentyltetrahydrothiophenium Tetraphenylborate: The product was obtained as a white solid (0.8 g, 93%). ^{1}H–NMR: (500 MHz, CD_3CN, 298 K): δ 0.92 (t, $^3J_{HH}$ = 7.1 Hz, CH_3, 3H); 1.30-1.45 (m, CH_2, 4H); 1.70 (p, $^3J_{HH}$ = 7.6 Hz, CH_2, 2H); 2.11–2.27 (m, $(CH_2)_2$, 4H); 2.95 (t, $^3J_{HH}$ = 7.4 Hz, CH_2, 2H); 3.10–3.21 (m, $(CH)_2$, 2H); 3.29–3.42 (m, $(CH)_2$, 2H); 6.86 (t, $^3J_{HH}$ = 7.2 Hz, $(CH)_{para}$, 4H); 7.01 (t, $^3J_{HH}$ = 7.4 Hz, $(CH)_{meta}$, 8H); 7.20-7.34 (m, $(CH)_{ortho}$, 8H). ^{13}C-NMR: (125 MHz, CD_3CN, 298 K): δ 14.00 (CH_3); 22.69 (CH_2); 25.51 (CH_2); 29.27 (CH_2); 30.87 (CH_2); 42.94 (CH_2); 44.15 (($CH_2)_2$); 122.82 (C_{para}); 126.81 (C_{meta}); 136.81 (C_{ortho}); 164.80 ($^1J_{CB}$ = 49 Hz, C_{ipso}). Elemental analysis [%] calc. for $C_{33}H_{39}SB$: C: 82.83%, H: 8.21%, S: 6.70%; Found: C: 82.91%, H: 8.07%, S: 6.56%. Melting point: 192 °C TGA (5 K·min^{-1}): decomp. (T_{onset}): 230 °C.

1-Hexyltetrahydrothiophenium Tetraphenylborate: The product was obtained as a white solid (0.81 g, 95%). ^{1}H–NMR: (500 MHz, CD_3CN, 298 K): δ 0.91 (t, $^3J_{HH}$ = 7.0 Hz, CH_3, 3H); 1.24-1.47 (m, CH_2, 6H); 1.69 (p, $^3J_{HH}$ = 7.5 Hz, CH_2, 2H); 2.10–2.27 (m, $(CH_2)_2$, 4H); 2.95 (t, $^3J_{HH}$ = 7.8 Hz, CH_2, 2H); 3.11–3.22 (m, $(CH)_2$, 2H); 3.30–3.41 (m, $(CH)_2$, 2H); 6.85 (t, $^3J_{HH}$ = 7.1 Hz, $(CH)_{para}$, 4H);

7.01 (t, $^3J_{HH}$ = 7.4 Hz, $(CH)_{meta}$, 8H); 7.20-7.35 (m, $(CH)_{ortho}$, 8H). ^{13}C-NMR: (125 MHz, CD_3CN, 298 K): δ 14.23 (CH_3); 23.03 (CH_2); 25.76 (CH_2); 28.45 (CH_2); 29.27 (CH_2); 31.71 (CH_2); 42.95 (CH_2); 44.15 (($CH_2)_2$); 122.81 (C_{para}); 126.81 (C_{meta}); 136.80 (C_{ortho}); 164.86 ($^1J_{CB}$ = 49 Hz, C_{ipso}). Elemental analysis [%] calc. for $C_{34}H_{41}SB$: C: 82.91 %, H: 8.39 %, S: 6.51 %; Found: C: 83.02 %, H: 8.17 %, S: 6.27 %. Melting point: 166 °C TGA (5 K·min^{-1}): decomp. (T_{onset}): 228 °C.

1-Heptyltetrahydrothiophenium Tetraphenylborate: The product was obtained as a white solid (0.78 g, 94 %). ^{1}H–NMR: (500 MHz, CD_3CN, 298 K): δ 0.91 (t, $^3J_{HH}$ = 7.0 Hz, CH_3, 3H); 1.23-1.45 (m, CH_2, 8H); 1.68 (p, $^3J_{HH}$ = 7.5 Hz, CH_2, 2H); 2.07–2.25 (m, $(CH_2)_2$, 4H); 2.92 (t, $^3J_{HH}$ = 7.6 Hz, CH_2, 2H); 3.08–3.18 (m, $(CH)_2$, 2H); 3.28–3.38 (m, $(CH)_2$, 2H); 6.86 (t, $^3J_{HH}$ = 7.2 Hz, $(CH)_{para}$, 4H); 7.01 (t, $^3J_{HH}$ = 7.4 Hz, $(CH)_{meta}$, 8H); 7.22-7.34 (m, (–CH)$_{ortho}$, 8H). ^{13}C-NMR: (125 MHz, CD_3CN, 298 K): δ 14.34 (CH_3); 23.26 (CH_2); 25.81 (CH_2); 28.75 (CH_2); 29.23 (CH_2); 29.27 (CH_2); 32.19 (CH_2); 42.95 (CH_2); 44.15 (($CH_2)_2$ (I)); 122.83 (C_{para}); 126.63 (C_{meta}); 136.82 (C_{ortho}); 164.88 ($^1J_{CB}$ = 49 Hz, C_{ipso}). Elemental analysis [%] calc. for $C_{35}H_{43}SB$: C: 82.98 %, H: 8.56 %, S: 6.33 %; Found: C: 83.23 %, H: 8.23 %, S: 6.11 %. Melting point: 129 °C. TGA (5 K·min^{-1}): decomp. (T_{onset}): 228 °C.

1-Octyltetrahydrothiophenium Tetraphenylborate: The product was obtained as a white solid (0.76 g, 95 %). ^{1}H–NMR: (500 MHz, CD_3CN, 298 K): δ 0.90 (t, $^3J_{HH}$ = 7.0 Hz, CH_3, 3H); 1.23-1.46 (m, CH_2, 10H); 1.71 (p, $^3J_{HH}$ = 7.5 Hz, CH_2, 2H); 2.13–2.29 (m, $(CH_2)_2$, 4H); 2.99 (t, $^3J_{HH}$ = 7.5 Hz, CH_2, 2H); 3.16–3.25 (m $(CH)_2$, 2H); 3.36–3.45 (m, $(CH)_2$, 2H); 6.85 (t, $^3J_{HH}$ = 7.2 Hz, $(CH)_{para}$, 4H); 7.00 (t, $^3J_{HH}$ = 7.4 Hz, $(CH)_{meta}$, 8H); 7.23-7.30 (m, $(CH)_{ortho}$, 8H). ^{13}C-NMR: (125 MHz, CD_3CN, 298 K): δ 14.37 (CH_3); 23.34 (CH_2); 25.79 (CH_2); 28.78 (CH_2); 29.27 (CH_2); 29.50 (CH_2); 29.65 (CH_2); 32.46 (CH_2); 42.96 (CH_2); 44.16 (($CH_2)_2$); 122.80 (C_{para}); 126.62 (C_{meta}); 136.80 (C_{ortho}); 164.86 ($^1J_{CB}$ = 49 Hz, C_{ipso}). Elemental analysis [%] calc. for $C_{36}H_{45}SB$: C: 83.05 %, H: 8.71 %, S: 6.16 %; Found: C: 83.24 %, H: 8.37 %, S: 5.93 %. Melting point: 108 °C. TGA (5 K·min^{-1}): decomp. (T_{onset}): 229 °C.

1-Nonyltetrahydrothiophenium Tetraphenylborate: The product was obtained as a white solid (0.75 g, 95 %). ^{1}H–NMR: (500 MHz, CD_3CN, 298 K): δ 0.93 (t, $^3J_{HH}$ = 7.0 Hz, CH_3, 3H); 1.25-1.458(m, CH_2, 12H); 1.74 (p, $^3J_{HH}$ = 7.5 Hz, CH_2, 2H); 2.17–2.32 (m, $(CH_2)_2$, 4H); 3.02 (t, $^3J_{HH}$ = 7.4 Hz, CH_2, 2H); 3.20–3.28 (m, $(CH)_2$, 2H); 3.39–3.48 (m, $(CH)_2$, 2H); 6.88 (t, $^3J_{HH}$ = 7.2 Hz, $(CH)_{para}$, 4H); 7.03 (t, $^3J_{HH}$ = 7.4 Hz, $(CH)_{meta}$, 8H); 7.25-7.34 (m, $(CH)_{ortho}$, 8H). ^{13}C-NMR: (125 MHz, CD_3CN, 298 K): δ 14.39 (CH_3); 23.39 (CH_2); 25.79 (CH_2); 28.77 (CH_2); 29.27 (CH_2); 29.54 (CH_2); 29.8 (CH_2); 29.93 (CH_2); 32.57 (CH_2); 42.96 (CH_2); 44.16 (($CH_2)_2$); 122.79 (C_{para}); 126.61 (C_{meta}); 136.80 (C_{ortho}); 164.85 ($^1J_{CB}$ = 49 Hz, C_{ipso}). Elemental analysis [%] calc. for $C_{37}H_{47}SB$: C: 83.12 %, H: 8.86 %, S: 6.00 %; Found: C: 83.14 %, H: 8.71 %, S: 5.81 %. Melting point: 116 °C. TGA (5 K·min^{-1}): decomp. (T_{onset}): 228 °C.

1-Decyltetrahydrothiophenium Tetraphenylborate: The product was obtained as white solid (0.75 g, 96 %). ^{1}H–NMR: (500 MHz, CD_3CN, 298 K): δ 0.90 (t, $^3J_{HH}$ = 6.2 Hz, CH_3, 3H); 1.20-1.45 (m, CH_2, 14H); 1.69 (p, $^3J_{HH}$ = 7.5 Hz, CH_2, 2H); 2.13–2.27 (m, $(CH_2)_2$, 4H); 2.96 (t, $^3J_{HH}$ = 7.8 Hz, CH_2, 2H); 3.13–3.23 (m, $(CH)_2$, 2H); 3.32–3.43 (m, $(CH)_2$, 2H); 6.85 (t, $^3J_{HH}$ = 7.2 Hz, $(CH)_{para}$, 4H); 7.00 (t, $^3J_{HH}$ = 7.4 Hz, $(CH)_{meta}$, 8H); 7.21-7.31 (m, $(CH)_{ortho}$, 8H). ^{13}C-NMR: (125 MHz, CD_3CN, 298 K): δ

14.41 (CH_3); 23.42 (CH_2); 25.80 (CH_2); 28.78 (CH_2); 29.27 (CH_2); 29.54 (CH_2); 29.98 (CH_2); 30.01 (CH_2); 30.36 (CH_2); 32.64 (($CH_2)_2$); 42.96 (CH_2), 44.16 (($CH_2)_2$); 122.81 (C_{para}); 126.61 (C_{meta}); 136.80 (C_{ortho}); 164.86 ($^1J_{CB}$ = 49 Hz, C_{ipso}). Elemental analysis [%] calc. for $C_{38}H_{49}SB$: C: 83.18 %, H: 9.00 %, S: 5.84 %; Found: C: 83.25 %, H: 8.91 %, S: 5.53 %. Melting point: 97 °C TGA (5 K·min^{-1}): decomp. (T_{onset}): 226 °C.

1-Butyltetrahydrothiophenium Bis(trifluoromethylsulfonyl) imide: The product was obtained as a highly viscous colorless liquid (68.2 g, 76 %). ^{1}H-NMR ($CDCl_3$, 500 MHz, 298 K): δ 0.97 (t, $^3J_{HH}$ = 7.3 Hz, CH_3, 3H); 1.51 (h, $^3J_{HH}$ = 7.3 Hz, CH_2, 2H); 1.76 (p, $^3J_{HH}$ = 7.6 Hz, CH_2, 2H); 2.31–2.40 (m, $(CH_2)_2$, 4H); 3.16 (t, $^3J_{HH}$ = 7.5 Hz, CH_2, 2H); 3.33–3.43 (m, $(CH)_2$, 2H); 3.53–3.66 (m $(CH)_2$, 2H). ^{13}C-NMR ($CDCl_3$, 125 MHz, 298 K): δ 12.93 (CH_3); 21.13 (CH_2); 26.95 (CH_2); 28.32 (($CH_2)_2$); 42.17 (CH_2); 43.18 (($CH_2)_2$); 119.76 (q, $(CF_3)_2$). Elemental analysis [%] calc. for $C_{10}H_{17}F_6NO_4S_3$: C: 28.2 %, H: 4.0 %, N: 3.3 %, S: 22.6 %; Found: C: 28.4 %, H: 4.1 %, N: 3.2 %, S: 22.8 %. TGA (5 K·min^{-1}): decomp. (T_{onset}): 275 °C.

1-Pentyltetrahydrothiophenium Bis(trifluoromethylsulfonyl) imide: The product was obtained as a highly viscous colorless liquid (55.7 g, 72 %). ^{1}H-NMR ($CDCl_3$, 300 MHz, 298 K): δ 0.86 (t, $^3J_{HH}$ = 7.1 Hz, CH_3, 3H); 1.28–1.44 (m, $(CH_2)_2$, 4H); 1.72 (p, $^3J_{HH}$ = 7.4 Hz, CH_2, 2H); 2.22–2.40 (m, $(CH_2)_2$, 4H); 3.10 (t, $^3J_{HH}$ = 7.5 Hz, CH_2, 2H); 3.24–3.39 (m, $(CH)_2$, 2H); 3.46–3.60 (m, $(CH)_2$, 2H). ^{13}C-NMR ($CDCl_3$, 75 MHz, 298 K): δ 13.45 (CH_3); 21.85 (CH_2); 24.88 (CH_2); 28.46 (CH_2); 29.95 (($CH_2)_2$); 42.50 (CH_2); 43.25 (($CH_2)_2$); 119.78 (q, $(CF_3)_2$). Elemental analysis [%] calc. for $C_{11}H_{19}F_6NO_4S_3$: C: 30.1 %, H: 4.4 %, N: 3.2 %, S: 21.9 %; Found: C: 30.4 %, H: 4.1 %, N: 3.1 %, S: 24.4 %. TGA (5 K·min^{-1}): decomp. (T_{onset}): 274 °C.

1-Hexyltetrahydrothiophenium Bis(trifluoromethylsulfonyl) imide: The product was obtained as a highly viscous colorless liquid (51.9 g, 74 %). ^{1}H-NMR ($CDCl_3$, 300 MHz, 298 K): δ 0.80 (t, $^3J_{HH}$ = 7.0, CH_3, 3H); 1.22–1.43 (m, $(CH_2)_3$, 6H); 1.68 (p, $^3J_{HH}$ = 7.5 Hz, CH_2, 2H); 2.17–2.37 (m, $(CH_2)_2$, 4H); 3.07 (t, $^3J_{HH}$ = 7.5 Hz, CH_2, 2H); 3.22–3.35 (m, $(CH)_2$, 2H); 3.44–3.57 (m, $(CH)_2$, 2H). ^{13}C-NMR ($CDCl_3$, 75 MHz, 298 K): δ 13.55 (CH_3); 22.03 (CH_2); 25.04 (CH_2); 27.50 (CH_2); 28.34 (CH_2); 30.73 (($CH_2)_2$); 42.38 (CH_2); 43.13 (($CH_2)_2$); 119.69 (q, $(CF_3)_2$). Elemental analysis [%] calc. for $C_{12}H_{21}F_6NO_4S_3$: C: 31.8 %, H: 4.7 %, N: 3.1 %, S: 21.2 %; Found: C: 32.1 %, H: 4.6 %, N: 3.1 %, S: 22.8 %. TGA (5 K·min^{-1}): decomp. (T_{onset}): 275 °C

1-Heptyltetrahydrothiophenium Bis(trifluoromethylsulfonyl) imide: The product was obtained as a highly viscous colorless liquid (14.0 g, 71 %). ^{1}H-NMR ($CDCl_3$, 500 MHz, 298 K): δ 0.83 (t, $^3J_{HH}$ = 6.8 Hz, CH_3, 3H); 1.24–1.29 (m, $(CH_2)_3$, 6H); 1.41 (p, $^3J_{HH}$ = 6.9 Hz, CH_2, 2H); 1.72 (p, $^3J_{HH}$ = 7.5 Hz, CH_2, 2H); 2.26–2.37 (m, $(CH_2)_2$, 4H); 3.11 (t, $^3J_{HH}$ = 6.9 Hz, CH_2, 2H); 3.26–3.37 (m, $(CH)_2$, 2H); 3.50–3.60 (m, $(CH)_2$, 2H). ^{13}C-NMR ($CDCl_3$, 125 MHz, 298 K): δ 13.84 (CH_3); 22.32 (CH_2), 25.26 (CH_2); 27.98 (CH_2); 28.43 (CH_2); 28.51 (CH_2); 31.28 (($CH_2)_2$); 42.67 (CH_2); 44.38 (($CH_2)_2$); 119.87 (q, $(CF_3)_2$). Elemental analysis [%] calc. for $C_{13}H_{23}F_6NO_4S_3$: C: 33.4 %, H: 5.0 %, N: 3.0 %, S: 20.6 %; Found: C: 33.6 %, H: 5.2 %, N: 2.9 %, S: 20.1 %. TGA (5 K·min^{-1}): decomp. (T_{onset}): 275 °C.

1-Octyltetrahydrothiophenium Bis(trifluoromethylsulfonyl) imide: The product was obtained as a highly viscous colorless liquid (41.12 g, 73 %). ^{1}H-NMR ($CDCl_3$, 500 MHz, 298 K): δ 0.84 (t, $^3J_{HH}$ = 6.6 Hz, CH_3, 3H); 1.24–1.45 (m, $(CH_2)_5$, 10H); 1.73 (p, $^3J_{HH}$ = 7.85 Hz, CH_2, 2H); 2.25–2.41 (m, $(CH_2)_2$, 4H); 3.12 (t, $^3J_{HH}$ = 7.6 Hz, CH_2, 2H); 3.28–3.40 (m, $(CH)_2$, 2H); 3.47–3.69 (m, $(CH)_2$, 2H). ^{13}C-NMR ($CDCl_3$, 125 MHz, 298 K): δ 14.01 (CH_3); 22.55 (CH_2); 25.33 (CH_2); 28.06 (CH_2); 28.56 (CH_2); 28.81 (CH_2); 28.83 (CH_2); 31.58 (($CH_2)_2$); 42.65 (CH_2); 43.36 (($CH_2)_2$). Elemental analysis [%] calc. for $C_{14}H_{25}F_6NO_4S_3$: C: 34.9 %, H: 5.2 %, N: 2.9 %, S: 20.0 %; Found: C: 35.6 %, H: 5.4 %, N: 2.5 %, S: 19.0 %. TGA (5 K·min^{-1}): decomp. (T_{onset}): 273 °C.

1-Nonyltetrahydrothiophenium Bis(trifluoromethylsulfonyl) imide: The product was obtained as a highly viscous colorless liquid (4.34 g, 70 %). ^{1}H-NMR ($CDCl_3$, 300 MHz, 298 K): δ 0.83 (t, $^3J_{HH}$ = 6.19 Hz, CH_3, 3H); 1.22–1.43 (m, $(CH_2)_6$, 12H); 1.71 (p, $^3J_{HH}$ = 7.58 Hz, CH_2, 2H); 2.23–2.39 (m, $(CH_2)_2$, 4H); 3.11 (t, $^3J_{HH}$ = 7.6 Hz,

CH_2, 2H); 3.27–3.37 (m, $(CH)_2$, 2H); 3.49–3.60 (m $(CH)_2$, 2H). ^{13}C-NMR ($CDCl_3$, 75 MHz, 298 K): δ 13.97 (CH_3); 22.54 (CH_2); 25.25 (−CH_2); 27.99 (CH_2); 28.48 (CH_2); 28.79 (CH_2); 28.99 (CH_2); 29.08 (CH_2); 31.69 (($CH_2)_2$); 42.55 (CH_2); 43.28 (($CH_2)_2$); 119.79 (q, $(CF_3)_2$). Elemental analysis [%] calc. for $C_{15}H_{27}F_6NO_4S_3$: C: 36.5 %, H: 5.6 %, N: 2.8 %, S: 19.4 %; Found: C: 36.6 %, H: 5.7 %, N: 2.8 %, S: 19.5 %. TGA (5 K·min^{-1}): decomp. (T_{onset}): 269 °C.

1-Decyltetrahydrothiophenium Bis(trifluoromethylsulfonyl) imide: The product was obtained as a highly viscous colorless liquid (52.74 g, 72 %). ^{1}H-NMR ($CDCl_3$, 600 MHz, 298 K): δ 0.84 (t, $^3J_{HH}$ = 6.9 Hz, CH_3, 3H); 1.16–1.33 (m, $(CH_2)_7$, 12H); 1.43 (p, $^3J_{HH}$ = 7.3 Hz, CH_2, 2H); 1.73 (p, $^3J_{HH}$ = 7.7 Hz, CH_2, 2H); 2.23–2.44 (m, $(CH_2)_2$, 4H); 3.13 (t, $^3J_{HH}$ = 7.7 Hz, CH_2, 2H); 3.30–3.38 (m, $(CH)_2$, 2H); 3.52–3.62 (m, $(CH)_2$, 2H). ^{13}C-NMR ($CDCl_3$, 150 MHz, 298 K): δ 14.09 (CH_3); 22.66 (CH_2); 25.35 (CH_2); 28.09 (CH_2); 28.57 (CH_2); 28.88 (CH_2); 29.20 (CH_2); 29.22 (CH_2); 29.37 (CH_2); 31.84 (($CH_2)_2$); 42.67 (CH_2), 43.38 (($CH_2)_2$); 119.85 (q, $(CF_3)_2$). Elemental analysis [%] calc. for $C_{16}H_{29}F_6NO_4S_3$: C: 37.7 %, H: 5.7 %, N: 2.8 %, S: 18.8 %; Found: C: 37.6 %, H: 5.6 %, N: 2.6 %, S: 19.2 %. TGA (5 K·min^{-1}): decomp. (T_{onset}): 275 °C.

Acknowledgements

This work has been supported by the German Research Foundation (DFG) in the framework of the priority program SPP 1708 "Material Synthesis Near Room Temperature" (grants VE 265–14/1 to SPV, HE 7165/7-1 for CH and JA 466/31-2 to CJ), as well as of the priority program SPP 1807 "*Control of London Dispersion Interactions in Molecular Chemistry*". DHZ acknowledges the financial support from DFG, grant ZA 872/3-1, 407078203. We thank Prof. G. Hägele for helpful discussions of the NMR spectra.

Conflict of Interest

The authors declare no conflict of interest.

Keywords: tetrahydrothiophene-based ionic liquids · PC-SAFT · vaporization enthalpies · vapor pressure · solubility

[1] J. S. Wilkes, M. J. Zaworotko, *J. Chem. Soc., Chem. Commun.* **1992**, 965–967.
[2] L. A. Balanchard, D. Hancu, E. J. Beckman, J. F. Brennecke, *Nature* **1999**, *399*, 28–29.
[3] P. Bonhôte, A.-P. Dias, N. Papageorgiou, K. Kalyanasundarum, M. Grätzel, *Inorg. Chem.* **1996**, *35*, 1168–1178.
[4] H. Tokuda, K. Hayamizu, K. Ishii, Md. A. B. H. Susan, M. Watanabe, *J. Phys. Chem. B* **2004**, *108*, 16593–16600.
[5] D. R. MacFarlane, P. Meakin, J. Sun, N. Amini, M. Forsyth, *J. Phys. Chem. B* **1999**, *103*, 4164–4170.
[6] J. Sun, M. Forsyth, D. R. MacFarlane, *J. Phys. Chem. B* **1998**, *102*, 8858–8864.
[7] Z.-B. Zhou, H. Matsumoto, K. Tatsumi, *Chem. Eur. J.* **2006**, *12*, 2196–2212.
[8] L. Guo, X. Pan, C. Zhang, M. Wang, M. Cai, X. Fang, S. Dai, *J. Mol. Liq.* **2011**, *158*, 75–79.
[9] Q. Zhang, S. Liu, Z. Li, J. Li, Z. Chen, R. Wang, L. Lu, Y. Deng, *Chem. Eur. J.* **2008**, *15*, 765–778.
[10] C. Xi, Y. Cao, Y. Cheng, M. Wang, X. Jing, S. M. Zakeeruddin, M. Grätzel, P. Wang, *J. Phys. Chem. C* **2008**, *112*, 11063–11067.
[11] M. Ma, K. E. Johnson, *Can. J. Chem.* **1995**, *73*, 593–598.
[12] H. Matsumoto, T. Matsuda, Y. Miyazaki, *Chem. Lett.* **2000**, *12*, 1430–1431.
[13] H. Matsumoto, H. Sakaebe, K. Tatsumi, *J. Power Sources* **2005**, *146*, 45–50.
[14] A. Orita, K. Kamijima, M. Yoshida, L. Yang, *J. Power Sources* **2010**, *195*, 6970–6976.
[15] D. Zhao, Z. Fei, W. H. Ang, P. J. Dyson, *Int. J. Mol. Sci.* **2007**, *8*, 304–315.
[16] L. Guo, X. Pan, M. Wang, C. Zhang, X. Fang, S. Chen, S. Dai, *Sol. Energy* **2011**, *85*, 7–11.
[17] J. Zhang, Y. Maa, F. Shi, L. Liu, Y. Deng, *Microporous Mesoporous Mater.* **2009**, *119*, 97–103.
[18] C. Jacob, G. I. Giles, N. M. Giles, H. Sies, *Angew. Chem.* **2003**, *115*, 4890–4907; *Angew. Chem. Int. Ed.* **2003**, *42*, 4742–4758.
[19] J. Gross, G. Sadowski, *Ind. Eng. Chem. Res.* **2001**, *40*, 1244–1260.
[20] A. Nann, C. Held, G. Sadowski, *Ind. Eng. Chem. Res.* **2013**, *52*, 18472–18481.
[21] C. Held, T. Reschke, S. Mohammad, A. Luza, G. Sadowski, *Chem. Eng. Res. Des.* **2014**, *92*, 2884–2897.
[22] M. Bülow, X. Ji, C. Held, *Fluid Phase Equilib.* **2019**, *492*, 26–33.
[23] M. Bülow, A. Danzer, C. Held, *in Encyclopedia of Ionic Liquids* (Eds. S. Zhang), Springer, Singapore, **2020**.
[24] L. Schmolke, S. Lerch, M. Bülow, M. Siebels, A. Schmitz, J. Thomas, G. Dehm, C. Held, T. Strassner, C. Janiak, *Nanoscale* **2019**, *11*, 4073–4082.
[25] A. Riisager, R. Fehrmann, M. Haumann, P. Wasserscheid, *Eur. J. Inorg. Chem.* **2006**, 695–706.
[26] R. Fehrmann, A. Riisager, M. Haumann, *Supported ionic liquids: fundamentals and applications*, WILEY-VCH Verlag, Weinheim, **2014**.
[27] H. Zhang, L. Yang, S. Fang, C. Peng, H. Luo, *Sci. Bull.* **2009**, *54*, 1322–1327.
[28] C. Rutz, L. Schmolke, V. Gvilava, C. Janiak, *Z. Anorg. Allg. Chem.* **2017**, *643*, 130–135.
[29] A. Schmitz, H. Meyer, M. Meischein, A. Garzón Manjón, L. Schmolke, B. Giesen, C. Schlüsener, P. Simon, Y. Grin, R. A. Fischer, C. Scheu, A. Ludwig, C. Janiak, *RSC Adv.* **2020**, *10*, 12891–128999.
[30] D. H. Zaitsau, A. V. Yermalayeu, V. N. Emel'yanenko, S. Butler, T. Schubert, S. P. Verevkin, *J. Phys. Chem. B* **2016**, *120*, 7949–7957.
[31] S. P. Verevkin, D. H. Zaitsau, V. N. Emel'yanenko, A. V. Yermalayeu, C. Schick, H. Liu, E. J. Maginn, S. Bulut, I. Krossing, R. Kalb, *J. Phys. Chem. B* **2013**, *117*, 6473–6486.
[32] D. H. Zaitsau, S. P. Verevkin, *J. Mol. Liq.* **2019**, *287*, 110959.
[33] S. P. Verevkin, *Struct. Chem.* **1998**, *9*, 113–118.
[34] V. Majer, V. Svoboda, H. V. Kehiaian, *Enthalpies of Vaporization of Organic Compounds: A Critical Review and Data Compilation*. Blackwell Scientific Publications, Oxford, **1985**.
[35] M. Bülow, D. H. Zaitsau, S. P. Verevkin, C. Held, *Chem. Open* **2020**, *in preparation*.
[36] X. Ji, C. Held, G. Sadowski, *Fluid Phase Equilib.* **2012**, *335*, 64–73.
[37] X. Ji, C. Held, G. Sadowski, *Fluid Phase Equilib.* **2014**, *363*, 59–65.
[38] M. Bülow, A. Schmitz, T. Mahmoudi, D. Schmidt, F. Junglas, C. Janiak, C. Held, *RSC Adv.* **2020**, *10*, 28351–28354.
[39] T. J. Wenzel, K. Cameron, *Magn. Reson. Biol.* 1989, 27, 734–739.
[40] Apex2, data collection program for the CCD area-detector system, SAINT, data reduction and frame integration program for the CCD area-detector system, Bruker analytical X-ray.
[41] G. Sheldrick, *Program SADABS: Area-detector absorption correction*, University of Göttingen, Germany, **1996**.
[42] G. M. Sheldrick, *Acta Crystallogr.* **2015**, A71, 3–8.
[43] G. M. Sheldrick, *Acta Crystallogr.* **2015**, C71, 3–8.
[44] DIAMOND 4 for Windows, Crystal Impact Gbr, Bonn, Germany; http://www.crystalimpact.com/diamond.
[45] S. P. Verevkin, D. H. Zaitsau, V. N. Emel'yanenko, A. Heintz, *J. Phys. Chem. B* **2011**, *115*, 12889–12895.
[46] G. Sauerbrey, *Z. Phys.* **1959**, *155*, 206–222.
[47] E. C. W. Clarke, D. N. Glew, *Trans. Faraday Soc.* **1966**, *62*, 539–547.

Manuscript received: August 14, 2020
Revised manuscript received: November 13, 2020